Electrically Enhanced Free Dendrite Growth in Polar and Non-polar Systems

Kenneth G. Libbrecht[1], Timothy Crosby, and Molly Swanson

Norman Bridge Laboratory of Physics, California Institute of Technology 264-33, Pasadena, CA 91125

[submitted to the Physical Review Letters, December 19, 2000]

PACS numbers: 68.70.+w, 81.30.Fb

Abstract. We describe the electrically enhanced growth of needle crystals from the vapor phase, for which there exists a morphological instability above a threshold applied potential. Our improved theoretical treatment of this phenomenon shows that the instability is present in both polar and non-polar systems, and we provide an extension of solvability theory to include electrical effects. We present extensive experimental data for ice needle growth above the electrical threshold, where at $T = -5$ C high-velocity shape-preserving growth is observed. These data indicate that the needle tip assumes an effective radius R^* which is nearly independent of both supersaturation and the applied potential. The small scale of R^* and its response to chemical additives suggest that the needle growth rate is being limited primarily by structural instabilities, possibly related to surface melting. We also demonstrate experimentally that non-polar systems exhibit this same electrically induced morphological instability.

The formation of stable spatial patterns is a fundamental problem in the study of nonlinear non-equilibrium systems [1], and controlling pattern formation has generated considerable recent interest in light of a host of possible technological applications. A now-standard example of a condensed-matter pattern-forming system is the diffusion-limited growth of free crystalline dendrites, which are nearly ubiquitous products of rapid solidification, from either liquid or vapor precursors. While the diffusion equation alone is sufficient to define a relationship between the dendrite tip velocity and tip radius, typically surface tension (which changes the surface boundary conditions via the Gibbs-Thomson mechanism) must be included in order to select a unique needle-like solution. Microscopic solvability theory has succeeded in furnishing a mathematically consistent and dynamically stable solution to this problem for simple 2D and 3D dendrite growth (ignoring, for example, surface kinetic and surface transport effects) [2, 3]. Instabilities and noise amplification leading to sidebranch generation have also been well studied.

In this Letter we examine shape-preserving needle growth from the vapor phase in the presence of an applied electrical potential. We previously described how high electric fields and field gradients near the needle tip can enhanced its growth, and subsequently drive in a new kind of growth instability for this system [4–7]. The growth behavior for small applied potentials is quite well described by an extension of solvability theory which we describe below. Above a threshold potential, however, the needle growth cannot be stabilized by the Gibbs-Thomson mechanism, and so the phenomenon lies outside the realm of solvability theory. We performed a series of experiments to examine needle growth in this new electric regime, where we can still observe shape-preserving growth, but with much increased tip velocities.. From these measurements we are able to infer the physical mechanisms responsible for controlling the enhanced needle growth rates.

We consider the case of diffusion-limited growth of a free crystalline dendrite, which is well known to exhibit a constant-velocity, needle-like solution with a parabolic tip geometry [3]. We will assume growth from the vapor phase, with low solute concentration in a non-polar solvent gas. When an electrical potential is applied to the growing crystal, the normal diffusion equation is replaced by

[1] Address correspondence to *kgl@caltech.edu*; URL: http://www.its.caltech.edu/~atomic/

the Smoluchowski equation [5, 8]

$$\frac{\partial c}{\partial t} = D\overrightarrow{\nabla} \cdot (\overrightarrow{\nabla} c + c\overrightarrow{\nabla}\Phi) \tag{1}$$

where c is the solute concentration, D is the diffusion constant, and the external force felt by the solute molecules is described as the gradient of the potential

$$\Phi = -\frac{\alpha}{kT}\left(\overrightarrow{E} \cdot \overrightarrow{E}\right) \tag{2}$$

where α is the molecular polarizability, and the electric field is the gradient of the electrical potential $\overrightarrow{E} = -\overrightarrow{\nabla}\varphi$ [5]. Ignoring interface kinetics, the continuity equation at the interface yields the normal component of the surface growth rate $v_n = (\widehat{n} \cdot \overrightarrow{v}_{surf})$ as

$$v_n = \frac{D}{c_{solid}}\widehat{n} \cdot (\overrightarrow{\nabla} c + c\overrightarrow{\nabla}\Phi)|_{surf} \tag{3}$$

where c_{solid} is the solid number density and the right-hand side is evaluated at the solidification front [8]. For our experiments the diffusion length $\ell_D \equiv 2D/v_n$ is very large compared to other length scales in the problem, so we can assume the slow-growth limit where $\partial c/\partial t$ can be taken equal to zero.

The boundary conditions in this problem are defined by the equilibrium vapor pressure above the crystal surface, which depends on the applied electrical potential, along with the vapor pressure at infinity, c_∞. For a spherical crystal with radius R a perturbation calculation yields the vapor pressure

$$c(R) \approx c_{sat}\left(1 + \frac{d_0}{R} - \frac{R_{es}^2}{R^2} + \frac{R_{pol}^2}{R^2}\right) \tag{4}$$

where c_{sat} is the equilibrium vapor pressure above a flat interface, $d_0 = 2\beta/c_{solid}kT$, β is the surface tension, $R_{es}^2 = \varepsilon_0\varphi_0^2/2c_{solid}kT$, $R_{pol}^2 = \alpha\varphi_0^2/kT$, and φ_0 is the applied potential [6]. The second term in the above expression is the usual Gibbs-Thomson effect [3], the third term arises from the electrostatic energy of a charged sphere, and the last term is present for polar molecules, since we are assuming zero field inside the crystal.

With these modifications to the diffusion equation and surface boundary conditions, we then obtain a modification of the Ivantsov equation relating the tip velocity, v, and tip radius, R, of a parabolic needle crystal [3, 5]

$$v \approx \frac{2D}{R\log(\eta_\infty/R)}\frac{c_{sat}}{c_{solid}}\left[\Delta_1 - \frac{d_0}{R} + C\frac{R_{elec}^2}{R^2}\right] \tag{5}$$

with

$$R_{elec}^2 = \frac{2\varepsilon_0}{c_{solid}}\frac{\varphi_0^2}{kT\log^2(\eta_\infty/R)} \tag{6}$$

where $\Delta_1 = (c_\infty - c_{sat})/c_{sat}$, $C = 1 + 2\gamma\alpha c_{solid}\Delta_1/\varepsilon_0$, and γ is a dimensionless geometrical constant. From the spherical growth problem, solved in the limit of small R_{elec} using a perturbation approach, we expect $\gamma \approx 0.2$. For $\varphi_0 = 0$ this becomes the slow-growth limit of the Ivantsov solution if we identify $\eta_\infty \approx \ell_D$. This result supersedes previous treatments [4–6] in which a cruder approximation was used, which effectively assumed $\gamma = 0$. For ice we find $C \approx 1 + 4.7\Delta_1$, and $R_{elec} \approx 40(\varphi_0/1000\text{ V})$ nm [9]; thus in our experiments described below the polarization term is larger than the electrostatic term. For unpolarized molecules $C = 1$.

In the absence of an applied potential solvability theory tells us that the small capillarity term, d_0/R, stabilizes the needle growth; the decrease in growth velocity for small R brought about by the Gibbs-Thomson effect opposes the Mullins-Sekerka instability [10]. The applied potential acts to increase the tip velocity for smaller R, thus tending to destabilize the growth. The electrical perturbation can be incorporated quite simply into solvability theory by defining a modified capillarity, $d_0' \equiv d_0 - CR_{elec}^2/R$, which then yields the new solvability relation

$$\sigma_0 = \frac{2d_0D}{vR^2}\frac{c_{sat}}{c_{solid}}\left(1 - C\frac{R_{elec}^2}{d_0R}\right) \tag{7}$$

where σ_0 is the solvability parameter in the absence of an applied potential. Combining this with the

Ivantsov relation then yields a quadratic equation for the tip radius, $R^2 - R_0 R + C R_0 R_{elec}^2/d_0 = 0$, where R_0 is the tip radius in the absence of an applied potential. This quadratic equation has no real roots for $R_{elec} > R_{elec,thresh} = (d_0 R_0/4C)^{1/2}$, implying that at above a threshold potential the Gibbs-Thomson effect can no longer stabilize needle growth.

Ice is a convenient experimental system in which to observe this phenomenon, and we previously described the behavior of ice needle growth for applied potentials at or below threshold [4–6]. The existence of a threshold potential was established, and the tip velocity as a function of φ_0 below threshold is described by the above theory (although there remain considerable theoretical uncertainties associated with the growth of faceted crystals). A principal aim of the experiments described here is to quantitatively examine the growth behavior above threshold, beyond the realm of solvability theory.

Our experiments were performed in air at atmospheric pressure, using a vertical diffusion chamber in which the supersaturation could be changed by adjusting the temperature profile within the chamber [5]. Crystals were grown on a thin wire substrate, to which an electrical potential could be applied. Supersaturation was determined using a combination of diffusion modeling and frost-point measurements, and we estimate an overall scaling uncertainty in our reported Δ_1 of roughly ± 30 percent.

Crystals grown at $T = -15$ C exhibited a classic dendritic morphology with growth along the a-axis, and the tip velocities were observed to increase approximately linearly with Δ_1 as shown in Figure 1(a). Above threshold at this temperature we nearly always observed the tip-splitting phenomenon described in [5]. Crystals grown at $T = -5$ C were needle-like, and at these high supersaturation levels the needle axis was typically displaced from the c-axis, with larger angular displacements toward the a-axis observed for larger Δ_1. Fits to these data using the Ivantsov relation yield tip radii of $R_0 \approx 1.2$ μm and 1.5 μm for $T = -15$ C and -5 C, respectively, independent of Δ_1. In both cases the data do not follow the trend $v \sim \Delta_1^2$ expected from solvability theory, at least over the limited range in Δ_1 shown here. This is probably because the crystals exhibit some faceting, implying that growth is limited by surface kinetics in addition to diffusion. Solvability theory does not extend to the faceted case, but we expect that the additional complication of facets will not affect our main results to a very large degree.

Above threshold the tip velocities of $T = -5$ C needles increased substantially, as is shown in Figure 1(c) and Figure 2. The threshold potential was found to be approximately 1000 volts, independent of Δ_1, implying $R_{elec,thresh} \approx 40$ nm. This is comparable to the expected $(d_0 R_0/4C)^{1/2} \approx 30(1 + 4.7\Delta_1)^{-1/2}$ nm (using $d_0 = 2$ nm and the R_0 inferred from our measurements). The quantitative agreement is satisfactory, but again the observations do not show the supersaturation dependence suggested by our simple solvability theory. From the supersaturation dependence at $\varphi_0 = 2000$ volts we find tip radii of $R^* \approx 360$ nm using the Ivantsov relation, again independent of Δ_1. These growth rates were observed to be the same (to ± 15 percent) for positive and negative applied potentials.

Adding trace quantities of certain chemical additives to the air in our diffusion chamber changed the electric needle growth dramatically, as shown in Figure 1(c). Under certain conditions the electric needles then grew along the c-axis, with velocities approximately four times faster than without additives, whereas there was no perceptible change to the normal crystal growth [11]. This chemically and electrically mediated growth as a function of φ_0 was qualitatively similar to the behavior shown in Figure 2 scaled by a factor of four, but the needle-to-needle scatter in the data was considerably greater. These data imply $R^* \approx 90$ nm at $\varphi_0 = 2000$ volts.

With these data in hand we can then examine possible physical mechanisms responsible for limiting the Mullins-Sekerka instability and producing shape-preserving growth at a constant tip velocity. Latent heat generated at the growing tip is a possible stabilizing mechanism, but it appears that the resulting thermal effects are not very important. Assuming heat generated by condensation is conducted along the needle and into the solvent gas, then the temperature rise at the tip is approximately $\Delta T \approx (\kappa_{solid}\kappa_{solvent})^{-1/2} L\rho v R$, where L is the latent heat and ρ is the solid density

[5]. Using the Ivantsov relation for vR, this becomes $\Delta T \approx 0.06\Delta_1$ °K. This temperature increase is small, and does not exhibit the strong R dependence needed to stabilize the tip growth.

Field emission can be examined using the Fowler-Nordheim relation, from which we estimate a current (for $\varphi_0 < 0$) of $I \approx 14\text{mA}\cdot(\varphi_0/1000\text{ V})^2 \exp\left[-310(R/1\ \mu\text{m})(1000\text{ V}/|\varphi_0|)\right]$. Assuming a power $P \sim I\varphi_0$ is deposited at the needle tip (likely an overestimate), and assuming the same simple conduction model as above, we estimate that tip heating becomes significant for $I \gtrsim 10^{-11}$ A. Ice surface conductance is high enough [12] that such low currents produce a negligible voltage drop along a needle.

We measured the current emitted from growing needle crystals, for which there is a considerable dependence on the sign of the applied potential. For $\varphi_0 = 2000$ volts we find $I < 1$ pA in clean air and $I \approx 1$ pA for chemically mediated growth (with considerable scatter in the latter measurements). For $\varphi_0 = -2000$ volts we measure $I \approx 1 - 3$ pA without additives and $I \approx 10$ pA with additives (again with considerable scatter). When $I \gtrsim 10$ pA we observe that the needle growth slows substantially, and the tip velocities become quite variable from needle to needle. We conclude that field emission plays a significant role when $\varphi_0 \lesssim -1000$ V and the crystals are grown in the presence of chemical additives, which results in sizable currents. In all other circumstances it appears field emission does not limit the needle growth.

Having eliminated thermal and field emission mechanisms, we propose that the electric needle growth is stabilized by the diminished structural integrity of the material when formed into an extremely sharp tip. That is, the needle tip radius becomes so small that its solid structure is unstable and subject to deformation driven by surface tension over timescales comparable to the crystal growth time $\sim R/v$. There is considerable uncertainty in our understanding of the structural properties of ice, however, particularly for such extremely small crystals, which makes detailed calculations difficult [12]. Surface melting certainly sets a lower bound on tip radius, since surface melting is known to produce a quasiliquid layer at these temperatures, which likely has very little resistance to shear stresses. The ice quasiliquid layer has a thickness of roughly 20 nm at $T = -5C$ [13], which is not insignificant compared to the tip radii inferred from our measurements.

One feature of our data that is readily explained by this model is that the measured tip radius R^* is essentially independent of Δ_1 and φ_0 in the electric growth regime (at least above a Δ_1-dependent transition region; see Figure 2). Above the threshold potential the tip radius decreases and the tip velocity increases to the point that structural deformations become a dominating influence. This must occur at some material-determined size scale, so we would expect that the new tip radius would depend mainly on material properties, and would not depend strongly on supersaturation or the applied potential, as is observed. The change in R^* in the presence of additives could be explained by the strongly anisotropic structural properties of ice, since the most rapid growth observed is for c-axis needles. We see that this stabilization mechanism is a distinct, more direct, manifestation of surface tension. While normal needle growth is stabilized by the increased vapor pressure over surfaces with large curvature—the Gibbs-Thomson mechanism—electric needle growth is stabilized by structural deformations brought about by surface tension in the sharp tip.

In a separate experiment, we also examined the electric growth phenomenon for a non-polar molecular solid by examining the growth of iodine crystals from the vapor. At a supersaturation of $\Delta_1 \approx 0.1$ we obtained the results shown in Figure 3. Rapid needle growth above a threshold potential of $\varphi_0 \approx 1000$ volts was clearly observed, although there was considerable scatter in the data. These data provide qualitative support of the above theory, and clearly verify that this morphological instability is present in non-polar systems.

In summary, we have examined the detailed physics of electrically enhanced needle crystal growth from the vapor phase. We find that an extension of solvability theory explains the existence of a threshold applied potential, φ_{thresh}, and adequately reproduces the magnitude of φ_{thresh} as well as the needle growth behavior for $\varphi_0 < \varphi_{thresh}$. For $\varphi_0 > \varphi_{thresh}$ we observed high-velocity growth of ice and iodine needle crystals, demonstrating that this new growth instability is indeed present in both polar and non-polar systems. Extensive measurements with ice suggest that electric needle growth in this system is usually not limited by the effects of latent heat deposition or field emission,

but appears to be limited by structural deformation of the needle tip. Additional experiments with other materials would further elucidate this process. In particular, since ice is a relatively soft material [12], these investigations suggest that harder materials could yield much sharper tips. Related experiments with refractory metals have yielded electric needle crystals with nanometer-scale tips [14], and we believe that additional research into electrically enhanced growth may lead to useful applications.

[1] For reviews see E. Ben-Jacob, *Cont. Phys.* **38**, 205 (1997); *Cont. Phys.* **34**, 247 (1993); J. S. Langer, in *Chance and Matter: Les Houches Session XLVI* (Elsevier: New York, 1987); H. Muller-Krumbhaar, in *Materials Science and Technology: a Comprehensive Treatment* (R. W. Cahn *et al.*, eds) (VCH: Weinheim, 1991); M. C. Cross and P. C. Hohenberg, *Rev. Mod. Phys.* **65**, 851 (1993).

[2] E. Brener, *Phys. Rev. Lett.* **71**, 3653 (1993); A. Karma and W. J. Rappel, *Phys Rev. Lett.* **77**, 4050 (1996)

[3] Y. Saito, *Statistical Physics of Crystal Growth* (World Scientific: Singapore) (1996), and references therein.

[4] K. G. Libbrecht and V. M. Tanusheva, *Phys. Rev. Lett.* **81**, 176 (1998).

[5] K. G. Libbrecht and V. M. Tanusheva, *Phys. Rev. E* **59**, 3253 (1999).

[6] E. A. Brener and H. Muller-Krumbhaar, *Phys. Rev. Lett.* **83**, 1698 (1999); K. G. Libbrecht and V. M. Tanusheva, *Phys. Rev. Lett.* **83**, 1699 (1999).

[7] J. T. Bartlett, A. P. van den Heuval, and B. J. Mason, *Z. angew. Math. Phys.* **14**, 599-610 (1963).

[8] S. Chandrasekhar, *Rev. Mod. Phys.* **15**, 1 (1943).

[9] These expressions contain the logarithmic divergence that is usually present for systems with cylindrical symmetry. The value of η_∞ in our experiments was determined by convection currents in our growth chamber, and was not well constrained. For numerical evaluations we take $\log(\eta_\infty/R) = 10$.

[10] W. W. Mullins and R. F. Sekerka, *J. Appl. Phys.* **34**, 323 (1963); J. S. Langer, *Rev. Mod. Phys.* **52**, 1 (1980).

[11] We discovered that certain volatile organic compounds, applied by injecting a small quantity of saturated vapor into the diffusion chamber, promote c-axis growth of electric needles at $T = -5$ C. We used a "cocktail" of VOCs for these experiments, for which we believe acetic acid was the principal active ingredient. Additive concentrations were estimated to be roughly at the part-per-million level in air. It appears that these additives are attracted by electric field gradients to the needle tip, which greatly enhances their effects compared to growth in the absence of an applied potential. We are currently studying the details of this process, and the results will be presented elsewhere.

[12] V. F. Pentrenko and R. W. Whitworth, *Physics of Ice* (Oxford University Press: Oxford) (1999).

[13] Based on glancing incidence X-ray diffraction, H. Dosch, A. Leid, and J. H. Bilgram, *Surf. Sci.* **327**, 145 (1995); other observational techniques indicate substantially different quasiliquid layer thicknesses [12].

[14] F. Okuyama, *Jpn. J. Appl. Phys.* **22**, 245 (1983); F. Okuyama, *Appl. Phys. A* **27,** 57 (1982).

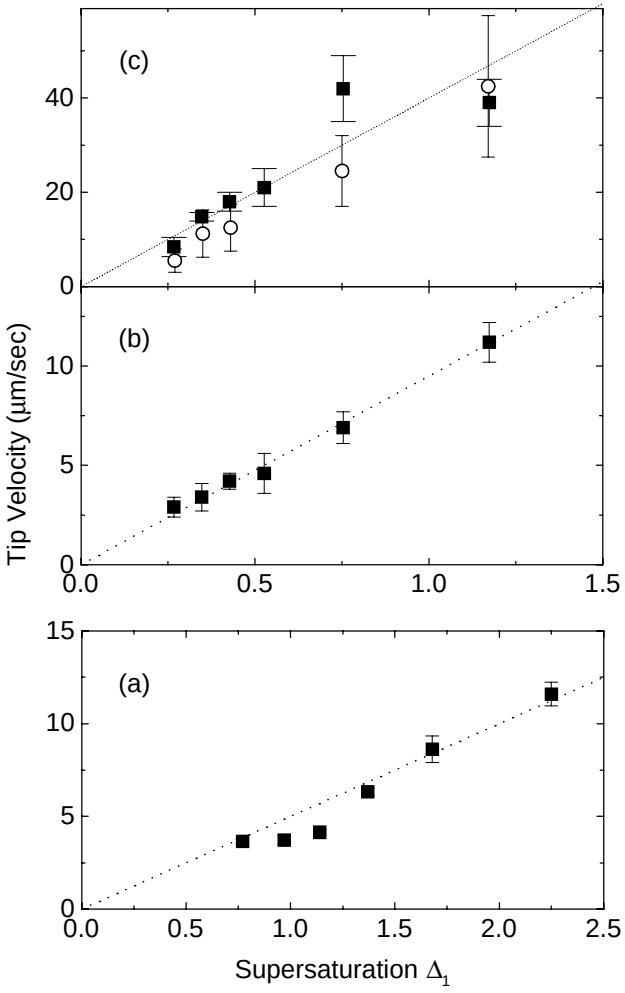

Figure 1. Tip velocities of growing ice needles, as a function of vapor supersaturation. (a) Dendrites grown at $T = -15$ C, with no applied potential; (b) Needle-like crystals grown at $T = -5$ C, again with no applied potential; (c) solid squares: v_{tip} for electric needles grown at $T = -5$ C with an applied potenial of 2000 volts; open circles: $v_{tip}/4$, for needles grown at $T = -5$ C and 2000 volts, but in the presence of vaporous chemical additives. These additives were used to promote growth along the c-axis, thus resulting in much faster growing needles.

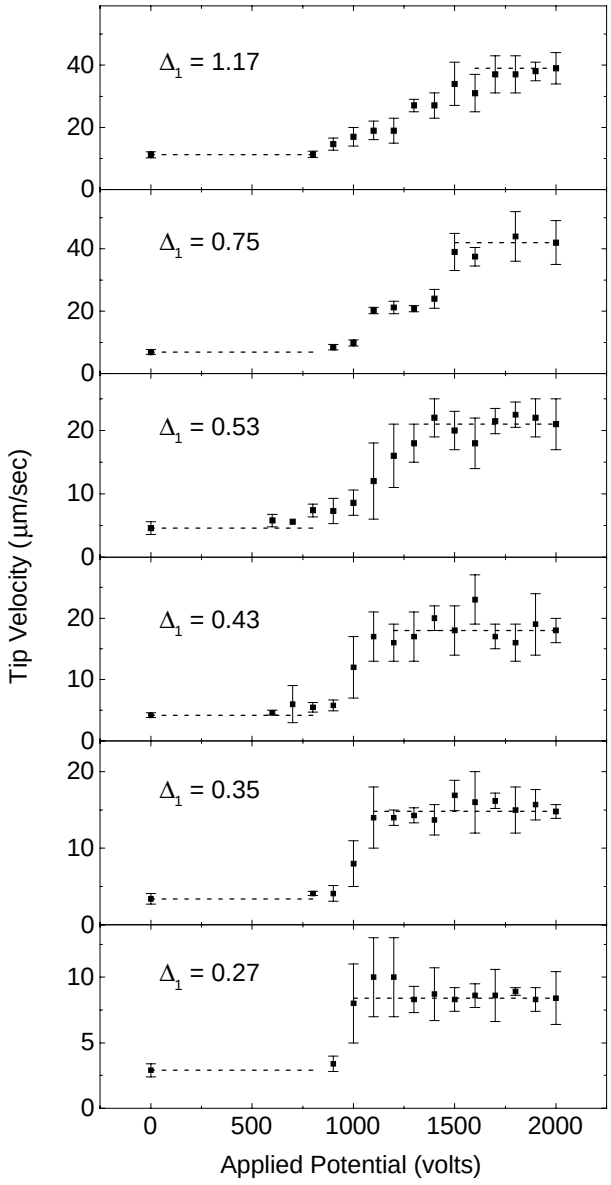

Figure 2. Tip velocities as a function of applied potential and supersaturation Δ_1, for ice needles grown at $T = -5$ C. Horizontal dotted lines were drawn through the first and last data points to guide the eye.

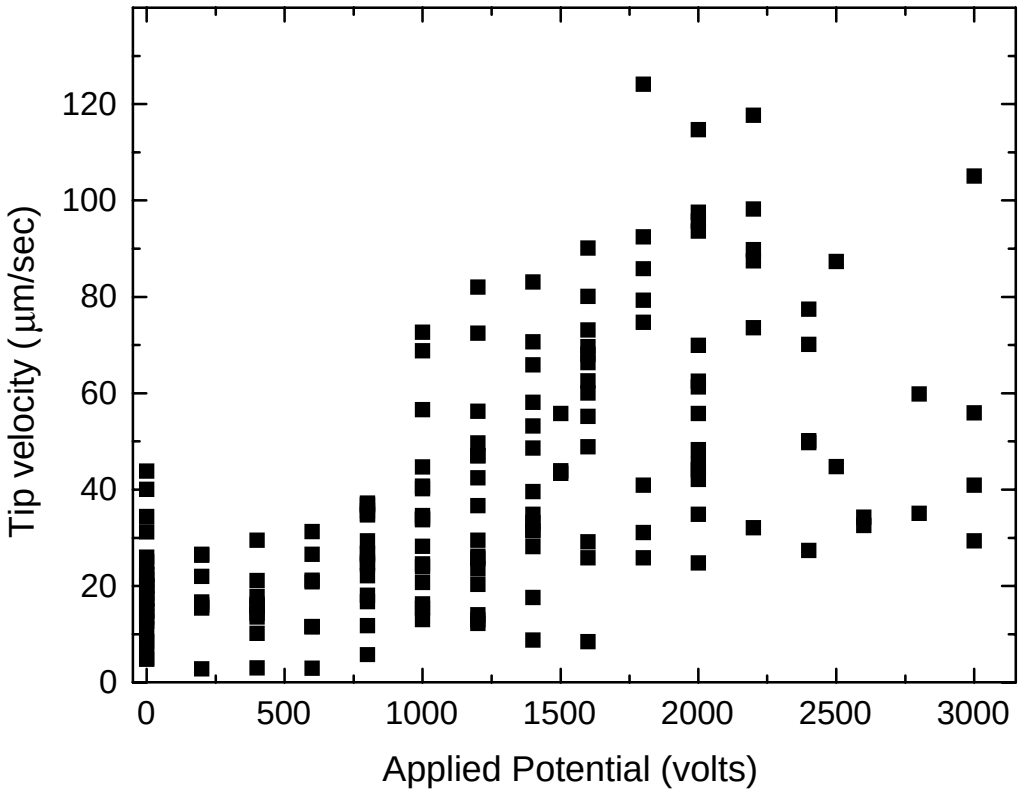

Figure 3. Tip velocities of growing iodine needle crystals as a function of the applied electrical potential. Each point represents the measurement of a single needle. Although the data show considerable scatter, there is clearly a large velocity increase above a threshold of ∼1000 volts, verifying the existence of this morphological instability for non-polar molecular systems.